JENS KNUDE

The Reddening at the North Galactic Pole

ABSTRACT. *Results from a recently completed photometric survey are presented. A complete sample of A5-G0 stars brighter than $V \sim 11.2$ mag and at latitudes above $b = +70°$ has been observed in the uvbyβ system.*

With an average of 4 stars deg^{-2} these data allow detailed studies of the local interstellar dust distribution at high latitudes.

The data obtained agree consistently with a previous uvbyβ investigation of polar A and F stars, Hill, Barnes and Hilditch. The mean E(b-y) difference, HBH-K, is only -0.005 ± 0.018 mag for 650 stars in common.

Substantial fractions of the north pole region are found to have color excesses larger than E(b-y) = 0.050 mag. The most reddened areas seem to be organized in longish features a few degrees wide and ten or more degrees long. The dust strings are parallel to the direction l: 37-217. Dust filaments are most frequent in the section $37 \lesssim l \lesssim 217$ but prominent structures also exist in the region $217 \lesssim l \lesssim 37$.

An irregular distribution of absorbing matter will influence counts of galaxies and clusters of galaxies and thus the angular distribution of these objects. As a first approximation to the effects caused by the presence of high latitude dust, the dust distributions angular autocorrelation function is computed for separations between adjacent lines of sight in the range from 10′ to 3 deg.

The dust is found to be uncorrelated in this sense. The autocorrelation function equals zero for the whole range of separations. Quite a surprising result because the autocorrelation of the gas column density distribution is a very clean exponential for $b > 40$ deg.

Assuming a constant ratio between gas and dust, which may not be a proper assumption, the clumping of the dust is studied in the context of a two component emission model for the diffuse soft X-ray background. The two component model is particularly interesting for high latitudes, where the proposed remote contribution originates in the halo. The effective absorption cross sections obtained from the best fits to the observed background in the B and C bands, Burrows et al., show a perfect agreement to the cross sections computed from the dust observations but deviates a factor two from those computed from the radio observations of the same regions. The radio and dust results lead to disagreeing conclusions on the existence of a hot halo. The dust distribution reconciles the soft background observations and the existence of a hot galactic halo.

Copenhagen University Observatory,
Øster Voldgade 3, DK-1350 Copenhagen K.

Introduction

Most fields of astronomy study physical processes where the radiation is influenced by the presence of solid material – dust. A particularly interesting part of the sky is the Galactic Poles, being the windows for extra galactic research, and because here the short lines of sight facilitate the study of individual interstellar structures.

The density structure of the interstellar matter with varying distance from the Galactic plane is important for understanding how it evolved and how it is energized. It is consequently a very serious problem that no consensus on the mere existence of high latitude dust has been reached. This disagreement implies several problems. As the distribution of dust is known only very fragmentary models are often adopted to correct for the reddening assumed to be present. This is the case in some extragalactic studies, where two models have been suggested. The most obvious model is a coherent plane parallel layer which results in a cosecant dependence of the estimated dust column on latitude; de Vaucouleur and Buta (1983) have reviewed the evidence for the plane layer concept. The sun may also be located in a sort of cavity in a plane layer of dust with a finite extent from the plane, Sandage (1973). The latter suggestion is a very attractive one because several bubble-like structures have recently been observed in the Galaxy. If such structures are frequent it is not unresonable that the sun could be inside one. If so should be the case many problems will find easier solutions because reddening corrections would only be required for low latitude objects beyond a few hundred parsecs and many calibrations would be facilitated and more accurate. A testing ground for the two concepts is the North Galactic Pole, NGP, where they disagree on the amount of matter present. The first model predicts substantial amounts of reddening, $E(B-V) \sim 0.05$ mag, whereas the second model estimates that no solid dust is present above latitude 50°.

In the search for high latitude dust some sort of a continuous background source is required. Variations in such a background could be interpreted as caused by absorbing matter. If faint galaxies have a homogeneous distribution the variation of their surface density with latitude may indicate whether matter is present or not. With a local cavity in a finite dust layer the surface density will level off at a certain latitude whereas the surface density will increase all the way to the pole in the first model. Counts of galaxies/clusters of galaxies are not able to set the zero point of the extinction but variations in the counts may

indicate the existence of matter at the poles. However, the counts are based on the assumption that the large scale distribution of luminous matter in the universe is homogeneous and isotropic – the fair sample hypothesis. There is also a disagreement on whether the counts of galaxies are too noisy, Burstein and Heiles (1978), to discriminate between a steadily increasing or a constant surface density above latitude 50°. The noise may depend on the reseau size used for the counts but may also contain some information on a variable absorption.

The problems mentioned lead naturally to ask how an irregular distribution of absorbing dust may influence the intrinsic distribution of galaxies. A recent study, using the Hat Creek 21 cm intensity, Seldner and Uson (1983), as an indicator for the dust, implies that if the dust is distributed analogous with the gas it may modify the intrinsic galaxy distribution significantly. The gas column densities have a correlated distribution and their autocorrelation obeys an exponential law. A correlated dust distribution may change the amplitude of the intrinsic power law distribution of galaxies and also reproduce the observed change of slope in the power law at separations $\sim 3°$. A mapping of the high latitude dust will naturally bear on this important problem.

The structure of the Galactic halo is most important in several respects. Here is only considered some aspects of the interstellar medium at the halo. Studies of ultraviolet absorption lines in LMC OB supergiants have revealed that the Galaxy has a hot $\sim 10^5$ K, high latitude plasma, Savage and de Boer (1981). Speculations on how interstellar clouds with high z-distances maintain pressure equilibrium suggest that a low density gas with even higher temperatures may confine such clouds, Spitzer (1956). The halo could contain substantial amounts of a 10^6 K gas which might be an important source of diffuse soft X-rays. With a soft X-ray halo and intervening neutral gas, intensity variations due to simple photoelectric absorption are to be expected in the background observations. On small angular scales the observations of the diffuse background are extremely smooth only showing variations on the 10% level. A global fit of soft X-ray count rates does however anticorrelate with the distribution of neutral hydrogen, McCammon et al. (1983). There is no straight forward explanation on this complex picture. Several models of the solar X-ray surroundings suggest that the dominating part of the X-ray emission originates within the nearest few $10^{19} \mathrm{cm}^{-2}$ of neutral hydrogen gas, Fried et al. (1980). In these models the background is virtually unabsorbed. Smooth intensity variations as observed are however also compatible with an extremely clumped spatial

distribution of an absorbing gas. It is possible to fit a two component emission model to the data: a local unabsorbed source and a remote absorbed. But an extreme clumping of the matter is required in order to reduce the efficiency of the absorption. In the modelling the effective absorption cross sections were taken as free parameters and the best fit values were found to be a factor of two lower than the computed atomic cross sections, McCammon et al. (1983). Continuum absorption of stellar light do not give any direct information on the gas clumping, only on the distribution of the solid component of the interstellar medium. Optical observations have however two advantages compared to most radio observations: an upper limit to the length of the dust column is given by the stellar distance and the optical beam is infinitely narrow without any side lobes. In principle the three dimensional distribution of the dust may result from the optical observations. If there is a constant – or known – ratio of gas to dust, the dust results may be applied to the gas distribution. But except, perhaps, for the cold gas, one still have to assume a constant ratio.

The influence of the diffusely dispersed dust on radiation has so far mostly been studied by its dimming and polarising effects on starlight. With the advent of the IRAS satellite more stringent investigations may be performed of the physical properties of the diffuse dust concentrations, because grain temperatures and compositions now may be brought into the discussion on an empiric basis. A promising field of research will be a combination of the dust observations as in the present study and the IRAS maps at 100μ. As the following discussion shows there is no unique spatial relationship between the amount of gas and dust but since significant patches of the NGP are much reddened one might expect fairly strong 100μ emission even though only minor amounts of neutral hydrogen is reported. The 100μ maps will probably have a streaked appearence as that displayed by the color excess distribution.

An observing programme

One of the exciting issues raised in interstellar studies is the structure of the interstellar medium (ISM) at the Galactic poles. Regarding the solid component of the interstellar matter (ism), it has long been questioned whether the optical data actually were related to the effects of intervening dust on radiation. Several photometric programmes have however indicated that matter is present but unfortunately about as many that it is

not. Some of the color excess catalogues were planned in a systematic way but often this has not been the case and the lines of sight were selected on a rather casual basis. It was therefore considered to be of some value to have a survey based on all stars of a given spectral range down to a rather faint limiting magnitude. The data forming the basis for the present study approximate the fulfilment of these requirements. Color excesses, E(b-y), for about 5000 lines of sight with $b > 70°$ were obtained.

E(b-y) measures the integrated dust column out to the star used as a background source. The whole idea to study the ism this way is based on a complete knowledge of the background sources' intrinsic continuum spectrum. Interstellar grains have a scattering cross section showing a λ^{-1} wavelength dependence in the optical, and is thus scattering the blue light more efficiently than the red. The continuum absorption results in apparent stellar colors redder than their intrinsic colors.

Accurate photometry is a must in interstellar studies. The gas density in the ISM is expected to be rather low: 10^{-2}-10^{+2} atoms cm^{-3} is the range anticipated in the diffuse medium. As the part of the interstellar space studied is within a few hundred pc, the expected gas columns are ranging from 6 10^{18} to 10^{21} atoms cm^{-2}. If the ism has a constant gas/dust ratio 7.5 10^{21} atoms mag^{-1}, Knude (1978), these columns translate to color excesses in the range from 0.001 to 0.13 mag. If columns with the smallest value are frequent the demands to the photometric accuracy are extreme. For fainter objects they can not be met presently. The best obtainable color excesses have a mean error $\sigma(E(b-y)) \lesssim 0.01$ mag. It has been proposed that the ism in the solar neighbourhood might be concentrated in small, still diffuse, clouds; if so, detailed observations are required for the detection of these features. If the ism on the other hand has a continuous distribution information on the dust distribution is obtainable from observations along a limited number of lines of sight. A principal objective of interstellar studies must be to find the characteristic linear scales of the mass concentrations. As a consequence observations must be performed in fine networks to ascertain a high detection probability even of the smaller features. Data samples representative of the ism consequently involve observations of several thousand stars.

The photometric system used by the author is the uvbyβ system by Strömgren (1966) and Crawford and Mander (1966). For interstellar purposes this system is presently calibrated for not too evolved population I stars of spectral type late A and for the whole F star range, Crawford (1975, 1978, 1979).

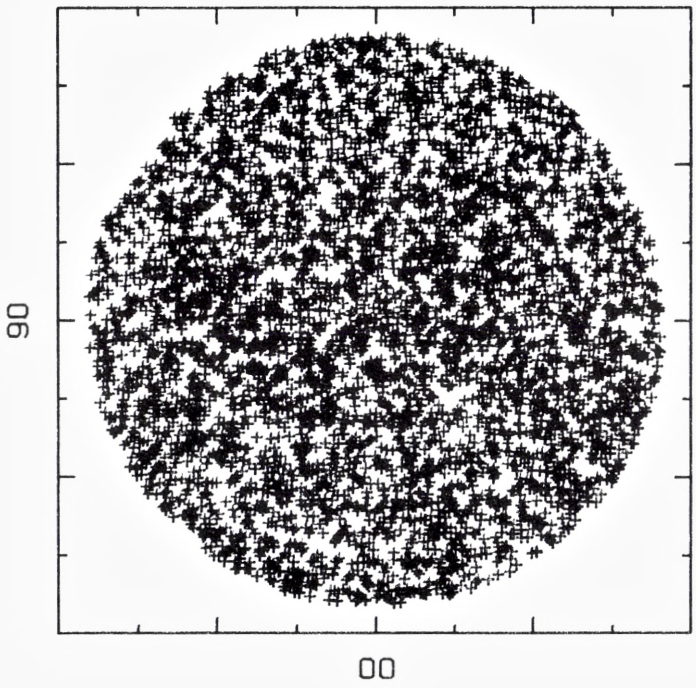

Fig. 1. Surface density of lines of sight where the color excess E(b-y) was measured. The smooth distribution is a contributory cause to assure an equal probability to observe identical dust features all over the polar cap, b > 70°.

For statistical computations an ideal network should have equal – and adjustable – spacings. The stellar distribution does of course not meet this demand, but as seen on Figure 1 the present sample has a fairly homogeneous distribution across the polar area.

When photometric surveys are planned the main obstacle is the scarcity of spectral cataloques from which candidate stars in the proper spectral range may be drawn. Candidate catalogues must further be complete in some respect either to a given limiting magnitude or to a limited distance range for subsequent evaluation of the completeness of the results obtained.

Spectral surveys of large areas are not abundant in the literature. It was therefore most fortunate that we learned that a rather deep, V ~ 11-11.5 mag, survey of the NGP was nearing completion, when the NGP programme was considered. The survey has been done by T. Oja, Uppsala, and was kindly put at the disposal of Professor B. Strömgren in the form of a handwritten catalogue containing 5458 entries.

Three problems remained before a photometric mapping of the dust distribution at the NGP could be attempted: accurate coordinates of the candidate stars which were identified either by a DM number or by

indicating the number of the nearest DM star, a suitable, efficient photometer and finally sufficient blocks of observing time on moderate sized telescope(s).

Coordinates were procured in collaboration with M. Winther, Institute of Astronomy, Aarhus University by using the Carte du Ciel Catalogues. The photometer, which was to become the prototype of a new generation six channel combination of the formerly used 4 and 2 channel uvby and Hβ photometers, was designed and built in the Brorfelde workshops of the Copenhagen University Observatory on a grant from the Carlsberg Foundation to B. Strömgren and P. E. Nissen. Generous amounts of observing time was granted on La Silla, Kitt Peak, Roque de los Muchachos and San Pedro Martir.

Finally the author had the pleasure of spending more than 180 observing nights on this particular programme between March 1, 1982 and May 15, 1984.

Heavy reddening at latitudes above +70°

As emphasized by Burstein and Heiles (1978), in the paper where the HI/GC method for reddening estimates is evaluated, only photometry of high latitude distant objects with well known intrinsic color may settle the dispute on the distribution and amplitude of the galactic pole reddening. The HI/GC method was calibrated on RR Lyrae stars and individual stars in globular clusters. Anyway the HI/GC reddening estimates are claimed to have an accuracy 0.010 mag in E(B-V) or 0.007 mag in E(b-y), comparable to the best obtainable intermediate band photometry, calibrated on local unreddened population I stars, with known metalictiy and evolutionary stage.

During the last few years new conclusions on the NGP reddening have been published. Hill, Hilditch and Barnes (1983) have presented a segmented reddening map of the NGP above b = 75°. Half of this region, l: 270-0-90, was found to have an average reddening E(b-y) = 0.008 mag, furthermore a small dust feature with E(b-y) = 0.024 mag was identified and found to coincide with a confined 21 cm feature on the maps by Heiles (1975). The stellar sample observed by HHB was drawn from the literature Hill, Barnes and Hilditch (1982). A list of common stars with DM numbers has been prepared and 650 stars from this sample have E(b-y) observations both by HHB and the present author. The

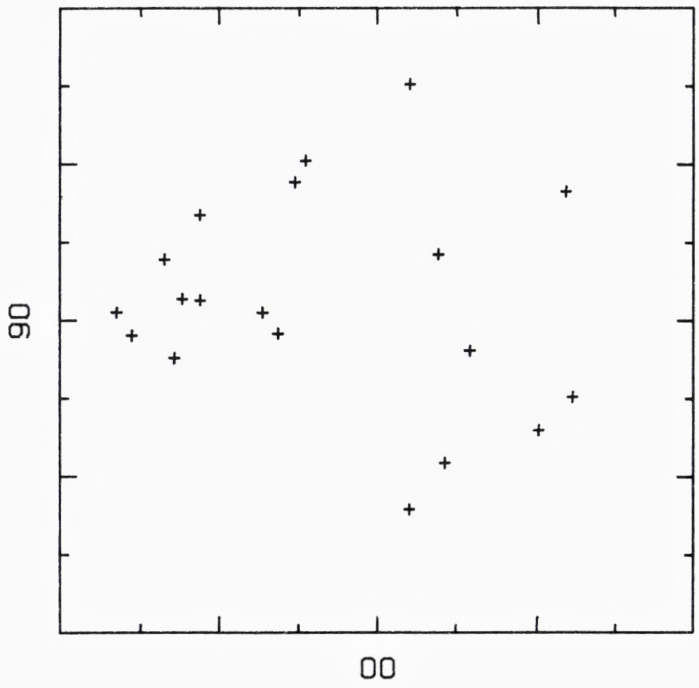

Fig. 2. Local heavily obscured regions in the polar direction. Lines of sight with color excesses measured to be above E(b-y) = 0.050 mag. The stellar background sources have photometric distances smaller than 100 pc. The dust seems to be confined to a filamentous structure. See also Fig. 3-8.

comparison of the photometry will be presented elsewhere. The mean difference of the color excesses $\langle E(b\text{-}y)_{HHB} - E(b\text{-}y)_K \rangle = -0.005$ mag with a standard deviation in the distribution of the residuals of only 0.018 mag. The common sample is made up mainly of F stars, for which Crawford (1975) quotes a standard deviation 0.012 mag of the color residuals for the basic calibrators assumed unreddened.

The programme has 75 stars in common with the Perry and Johnston (1982) reddening survey of the northern part of the volume within 300 pc. $\langle E(b\text{-}y)_{PJ} - E(b\text{-}y)_K \rangle = -0.014 \pm 0.014$. Perry and Johnston's sample is primarily A stars and their reddenings were reduced by Perry and Johnston by 0.009 mag in order to have identical mean reddenings for the F and for the A stars. If this reduction is not performed the mean difference will change to about −0.007 mag. There are hardly any significant zero point differences in the three samples. One might add – as was to be expected. Without the zero point amendment of the PJ sample the mean difference of the HHB and PJ sample becomes $\langle E(b\text{-}y)_{HHB} - E(b\text{-}y)_{PJ} \rangle = -0.003 \pm 0.015$ mag for 41 stars. Without the A star correction the reddening of the 90 Perry and Johnston stars above b = 70° is 0.007 mag, or E(B-V) = 0.010 mag. If it is permissible to use Burstein

and Heiles calibration formula in the reverse sense and further ignore the variable gas/dust ratio controlled by the galaxy counts, their equation four in the 1978 paper estimates an average HI column 2.9 10^{20} cm^{-2} from E(B-V) = 0.010, which is much larger than observed. Whether the amendment of Perry and Johnston's A star reddenings is a requisite or not is not evident.

From the NGP programme uvbyβ data for about 4800 stars are available for immediate computation of color excesses. Figure 1 shows the resulting distribution of lines of sight. The coverage is seen to be fairly homogeneous across the entire cap. Thus there is an identical probability to detect the effects of 'large scale' extinction features over the whole region. With four stars per square degree the average separation between adjacent lines of sight is 30' so quite small features may also be studied using this sample. A detailed discussion of absorbing material at the NGP is not attempted here, but some new discoveries are presented mostly as a picture gallery. As one of the most disputed questions has been the existence of substantial amounts of nearby absorbing material in the pole directions, Perry, Johnston and Crawford (1982), Figure 2 shows what may be termed as obscured local polar regions. Nearby is

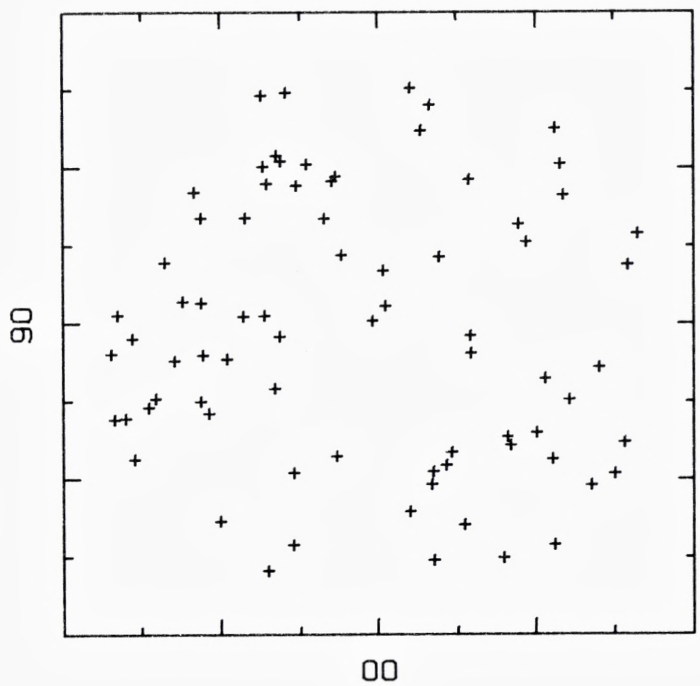

Fig. 3. Caption as to Fig. 2 except that this diagram has a lower reddening limit E(b-y) = 0.030 mag. The distance range is 0-100 pc.

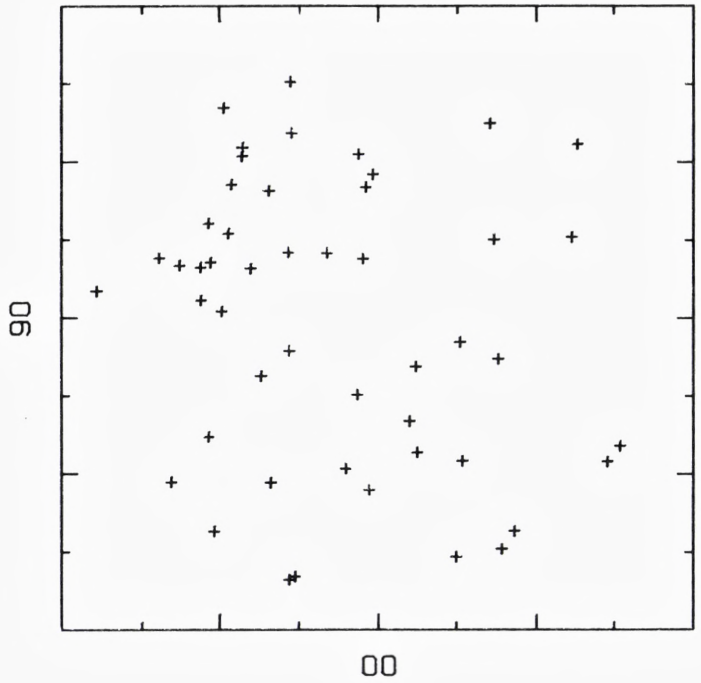

Fig. 4 Caption as to Figure 2 but for the distance range from 100 to 150 pc.

defined as within 100 pc, substantial reddening as a color excess beyond 0.050 mag. With almost any photometric accuray 0.050 mag is more than three sigmas above zero reddening. Most of the cap is free from such large local reddening. But even with these few points a clustering of the reddened directions is noticed. The high local excesses tend to concentrate in the quadrants l: 270°-360° and l: 90°-180°. Most local reddening is found at l~90° and b in the range from 70° to 80°. The distribution on Figure 2 may just indicate what is to become apparent for the more distant intervals, that the most reddened parts of the NGP is confined to filaments which stretch across the pole region. The dust filaments may be made up by smaller discrete features. In the galactic plane individual 'coherent' clouds with reddenings as small as 0.015 mag were found, Knude (1979). For comparison Figure 3 is a polar diagram of all directions with E(b-y) > 0.030 mag for the same distance interval as Figure 2. Note that all excesses > 0.050 are located in well confined 0.030 mag features. Two stars with E(b-y) > 0.030 mag and within 100 pc are located inside the 0.024 mag feature noted by Hill, Barnes and Hilditch (1983). The remaining dust structures on Figure 2 and 3 have not been seen previously. The appearence of the dust distribution is filamentous. The orientation of the threads on Figure 3 is not unambiguous. There are

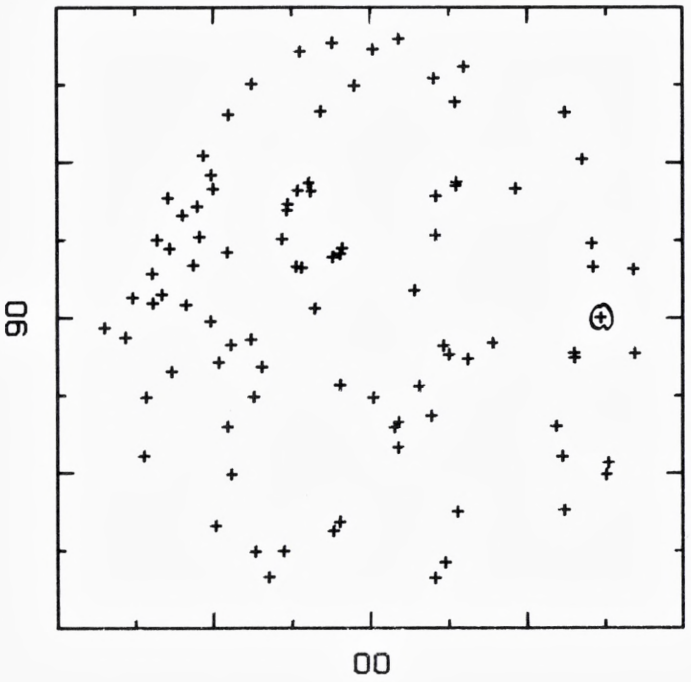

Fig. 5. Caption as to Figure 2 but for the distance range from 150 to 200 pc. The line of sight crossing Burstein and Heiles (1982) intensity maximum above latitude +70° is marked. Note the thready character of the distribution.

two clear, dust free lanes parallel to l: 55-235 but only in the l: 235-360-55 part of the cap. In the range l: 55-235 the preferred direction of the filaments is almost perpendicular to the direction 55-235. Figure 4 to 7 is a sequence of 50 pc wide distance segments – note *not* z-distances.

On Figure 4 is seen a clustering tendency in the distribution of excesses above 0.050 mag as on Figure 3 for the smaller excesses, but with a higher concentration of large excesses in the 90-180 quadrant. In the three remaining quadrants the distribution is filamentous. The distance range 150-200 pc is shown on Figure 5. Again a very prominent structure is seen near the rim for l: 90-120 and b: 70-73. It is difficult to tell whether the distribution is best conceived as a coherent entity or as a sequence of nearly parallel filaments stretching from the rim of the area towards the pole. As an example of the strong variations found the longitude 143 is considered. First there is some dust along the rim then a 5° wide void followed by a very sharp reddening ridge, then another void and again a sharp ridge and finally a clear region up to the pole. The reddening distribution for the stars in this distance interval is demonstrably thready. Figure 6, 200-250 pc, corroborates the thready tendency, but here the dust is concentrated almost exclusively in the longitude range from 37 to 217 degrees and confined to two dust bands parallel to

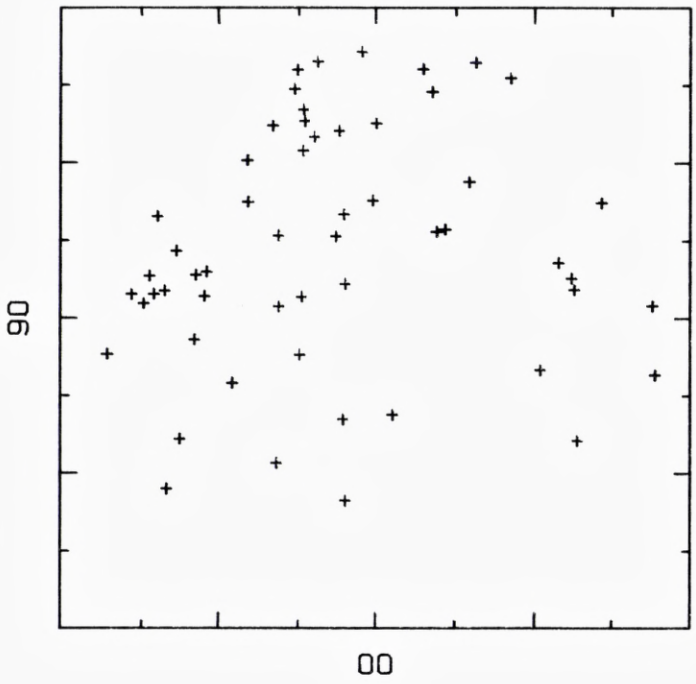

Fig. 6. Caption as to Figure 2. Distance range from 200 to 250 pc. The dust is almost exclusively found in the longitude range l: 45°-225°.

the 37-217 diagonal. Figure 7 is a very clean specimen of the filamentous general distribution. One has to conclude that the most reddened parts of the NGP are confined to filaments organized in a parallel pattern.

Finally Figure 8 displays the projected distribution of all lines of sight measured to have a color excess larger than E(b-y) = 0.050 mag. The projection is characterized by a broad, ~5° wide band almost without any heavy obscuration stretching across the entire cap including the pole itself. The distribution of the heavy reddening outside the clear path is indeed patchy but as suggested by the reddening distribution in the sequence of distance bins the reddening seems mostly to be found in string-like structures. The general direction of the system of strings is more or less lined up with the clear path l: 37-217. The strings may be made up by smaller structures some of which are oriented perpendicular to the general string direction. This 'clear' picture of the reddening distribution will be smoothed when the lesser reddenings are taken into account.

It is a surprise that the only feature in common to the HHB map is the curved feature delineated on Figure 8. Burstein and Heiles (1982), Figure 7(a), also show this feature in atomic hydrogen. Except for a few addi-

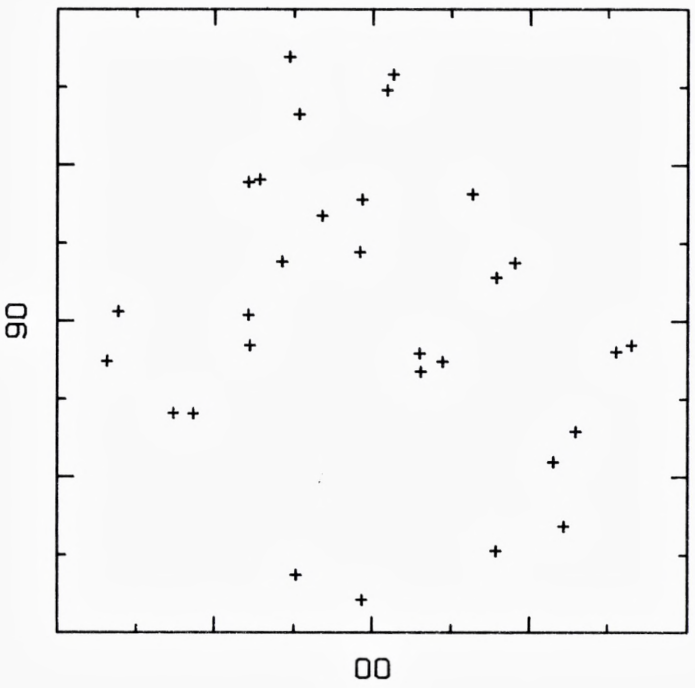

Fig. 7. Color excesses larger than E(b-y) = 0.050 mag for stars in the distance range from 250 to 300 pc. Note the very narrow dust filaments.

tional very small structures it is the only conspicuous HI entity above 70°. The maximum reddening estimate by the HI/GC method is at (l,b) = (270,74) and equals E(b-y) = 0.030 mag. A single line of sight with excess above 0.050 crosses this region. The distance to the dust is probably in the range from 150 to 200 pc. A most striking conclusion that follows from a comparison of Figure 8 to Figure 7 (a) of Burstein and Heiles (1982) is that there are indications of a large scale *anticorrelation* between the dust and the atomic gas distribution. Most of the heavily reddened regions are located in the section l: 30-210, which is the part of the polar cap where the lowest HI contours are located. An immediate qualitative result is to expect large variations in the ratio N(HI)/E(b-y) in this part of the sky. It is tentatively suggested that there may be extended regions at the NGP where dust exists without atomic gas.

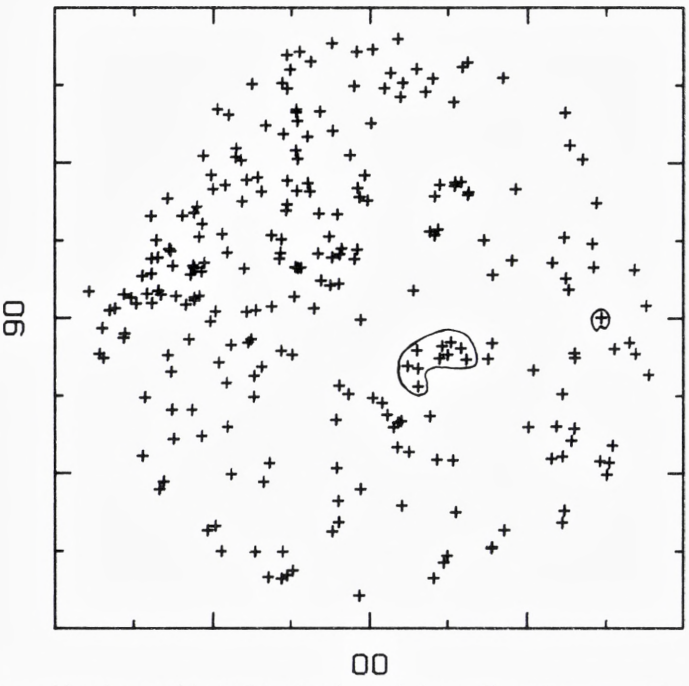

Fig. 8. Projected dust distribution for stars with $E(b-y) > 0.050$ mag. The only NGP dust feature reported previously is delineated. Burstein and Heiles intensity maximum is also indicated. The reddening distribution is characterized by a patch free from heavy obscuration stretching across the pole in the direction l: 37-217. There may be a tendency that the dust bands are oriented in the same direction. A qualitative comparison to 21 cm intensity maps indicates that the most reddened part of the NGP coincides with the smallest 21 cm intensities.

The autocorrelation function of high latitude dust

We have seen that the counts of galaxies have been used as an indicator of the variation of extinction with latitude at high latitudes and in the HI/GC method galaxy counts were further used as an estimator of changes in the ratio between gas and dust. Conversely the observed dust distribution will find applications in the study of the intrinsic galaxy clustering. Davis, Groth and Peebles (1977) conclude that the two-point correlation function is not seriously effected by variable extinction whereas Seldner and Uson (1983) try to explain the observed galaxy autocorrelation by a combination of an intrinsic unbroken power law and clumped galactic obscuration represented by the HI column density distribution.

The angular autocorrelation function has been computed for several cataloques of galaxy counts and is found to obey a combination of two power laws where the change of power occurs at an angular separation at about 3°. It is an important problem whether the amplitude and the power is a consequence of local galactic obscuration or they represent properties of the intrinsic galaxy distribution. The intrinsic galaxy distribution is assumed to be a power law. The galactic extinction may be important because the probability, dp, to observe a galaxy with apparent magnitude, m, in the range m, m+dm, within a solid angle $d\Omega$ in a direction (l,b) depends on the absorption in this direction:

$$dp(m,l,b) = d\Omega dm \int_0^\infty r^2 dr\ \Phi(m - 5 \log r - 5 - A(l,b))$$

Φ is the galaxy luminosity function, A(l,b) the absorption out of the Galaxy in the direction (l,b). Catalogues of deep galaxy counts are often presented as a listing of a surface density of galaxies as a function of position. What is counted is mostly the number of galaxies brighter than certain limiting magnitudes within a given solid angle. Obscuration has several effects on galaxy counts, either it dims a galaxy so much that it falls below the detector threshold or also the appearance of the galaxy is modified so it can not be discriminated from a stellar object. Only the first effect is considered here: a galaxy with a certain luminosity is only counted if its distance and the obscuration place it above the catalogues' limiting magnitude, m_o

$$dp = d\Omega_1 \int_0^\infty O(A,l,b) dA \int_{-\infty}^{m_o - A} dm \int_0^\infty r^2\ dr\ \Phi(m - 5 \log r - 5)$$

where O(A)dA is the probability to encounter an obscuration in the range A,A+dA in the direction (l,b). O(A) is not known as a function of galactic coordinates. The probability to have a simultaneous sighting of two galaxies brighter than m_o in two directions separated by an angle Θ_{12} is similarly

$$dp = d\Omega_1 d\Omega_2 \int_0^\infty \int_0^\infty O_{12}(A_1, A_2, \Theta_{12})$$
$$\int_{-\infty}^{m_o - A_1} dm_1 \int_{-\infty}^{m_o - A_2} dm_2 \int_{-\infty}^{\infty} \int_0^\infty r_1^2 dr_1 r_2^2 dr_2$$
$$(\Phi(m_1 - 5 \log r_1 - 5) \cdot \Phi\ (m_2 - \log r_2 - 5) + \text{cross term})$$

$O_{12}(A_1,A_2,\Theta_{12})$ is the joint probability to observe the absorptions A_1 and A_2 along two lines of sight separated by Θ_{12}. The frequency function $O_{12}(A_1,A_2.\Theta_{12})$ is also quite unknown.

However, the functions O(A) and $O_{12}(A_1,A_2.\Theta_{12})$ can be estimated for the zone above b = 70° by using the ~5000 E(b-y) values. In fact these distribution functions are not required to be known in details for evaluating the influence of absorption on the clustering of galaxies. If the amplitude of the extinction is small the luminosity function may be expanded in powers of the absorption. For small absorptions only the first and second order moments of the dust distribution are required.

The function O_{12} is the variation of the average of A_1A_2 with separation Θ. For $\Theta = 0$ the function is related to the number of clouds per unit length along a line of sight.

Sorting out the color excess data in preselected separation and color excess intervals consumes much computing time. Before complicating the analysis by binning in distance intervals etc. the autocorrelation was computed for the complete sample of NGP stars. The stars are thus not separated in distance bins before the average absorption products are computed. The effect of this simplification is not quite clear, but it may be of minor importance because a preliminary discussion of a subsample of NGP stars, Knude (1984), indicated that only minor variations of the dust distributions average properties are to be expected within the first 300 pc from the plane. One might think that this problem was easily solved by only including stars beyond a certain distance limit to make sure that the integrated column out of the plane was measured. But with a discrete distribution of the obscuration the most distant stars in magnitude limited samples, as the NGP sample, are only included because they happen to be unreddened. Exclusive use of the most distant stars will thus bias the reddening amplitude towards lower values. In the computation of the mean absorption products, separations from 10′ to 3° have been considered. Rim effects are corrected for by weighting pairs by the fraction of the annulus inside the zone b > 70°. The means are computed for all excesses in the range from −0.030 to 0.100 mag. It is tacitly assumed that there is a constant ratio of selective to absolute absorption.

With preselected excess values, E_1 and E_2, excesses in the interval $E_1 \pm 0.005$ mag are combined to excesses in the range $E_2 \pm 0.005$ mag for the 18 separations 10′ +n 10′, n = 0,1,2,...,17. For a separation Θ the proper E_2's are searched after in an annulus $\Theta \pm 5'$. On Figure 9 the variations of the joint probability to find two excesses with a separation Θ are shown

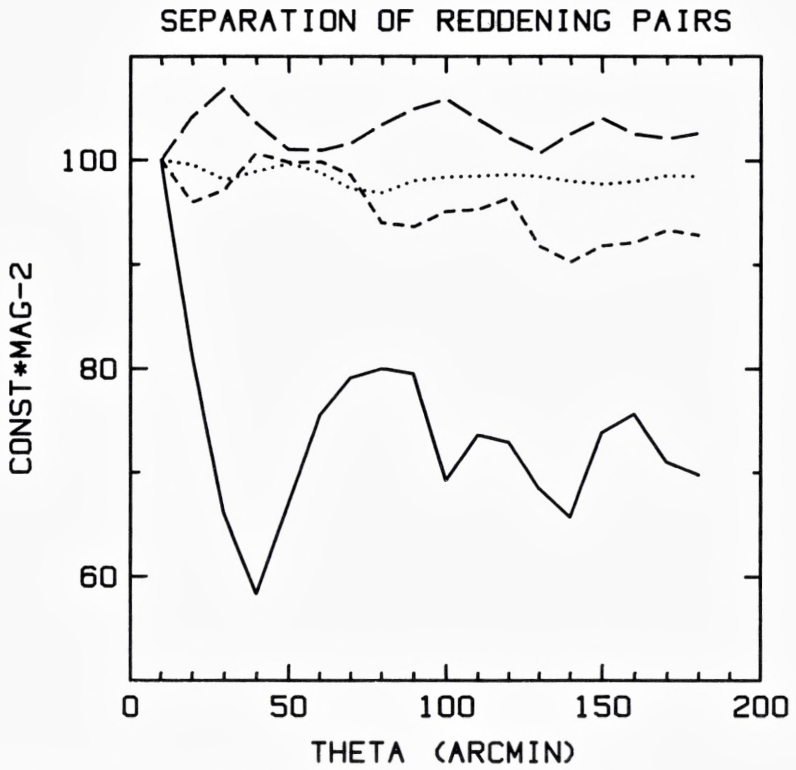

Fig. 9. Relative frequency of (E_1,E_2) pairs as a function of separation Θ.
(–0.020,–0.010) .....
(0.010, 0.020) — — — —
(0.020. 0.030) - - - - -
(0.030, 0.040) ————
The curves are shifted to a common origin. Note particularly the difference between the ICM curve (.....) and the cloud curve (————).

as a function of Θ. The scale is arbitrary and the curves have been shifted to a common origin. The curves shown are for the (E_1,E_2) pairs (− 20,-10),(10,20),(20,30),(30,40) in mmag. The two first pairs may be representative for the clear lines of sight and the two last for obscured lines of sight. The probability to have two clear lines of sight is thus constant for the whole range of separations considered. For the pairs (0.020,0.030) the joint probability shows a decreasing tendency with increasing separation. For the excess pairs (0.030,0.040) the decreasing tendency is confirmed. The decrease is however not monotonic but the joint probability indicates that these pairs are distributed on preferred angular scales. Separations below 20′, between 60′ and 100′, and between 150′ and 170′ are the most common.

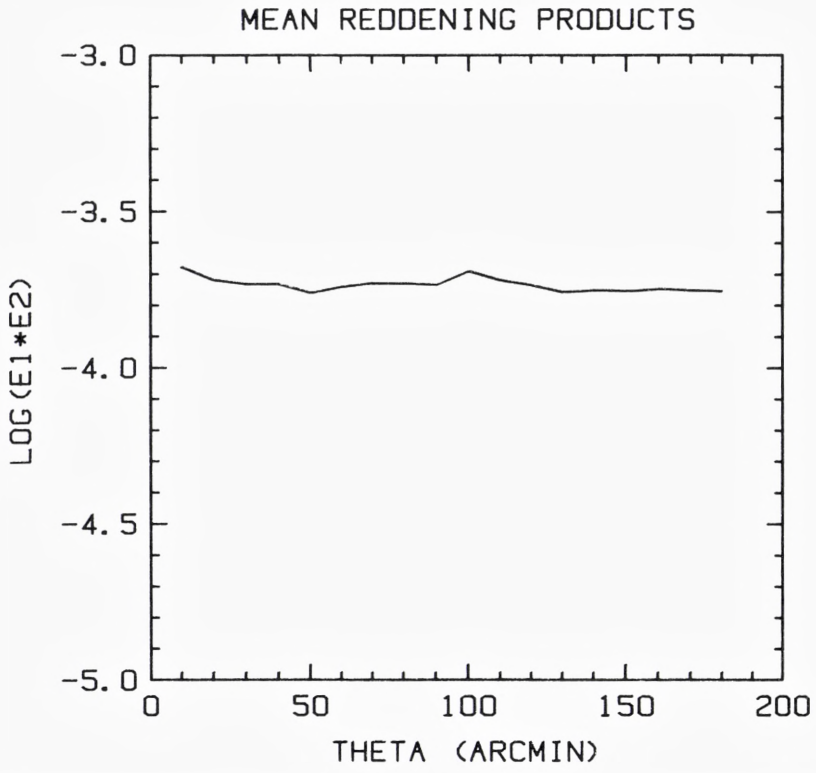

Fig. 10. Average excesses $\langle E_1E_2\rangle_\Theta$ as a function of separation. The average cross products are constant implying an uncorrelated dust distribution. The dust autocorrelation function, defined in the text, is accordingly ~0 unlike the N_H distribution which is a clean exponential.

Finally the products $E_1E_2O(E_1,E_2,\Theta_{12})$ are integrated over the observed excesses for constant Θ to obtain $\langle E_1E_2\rangle_\Theta$. The integral is computed for the 18 values of Θ considered. In the light of the neat dependence of the N(HI) autocorrelation on Θ the result for the dust is really unexpected, because the mean $\langle E_1E_2\rangle_\Theta$ does not show any dependence on separation whereas the HI columns follow an $\exp(-\Theta)$ law. The average products equal the ~mean square for the complete sample. With the definition of the autocorrelation function

$$\omega_E(\Theta) \equiv \langle E_1E_2\rangle_\Theta / \langle E\rangle^2 - 1 \simeq 0,\ \Theta \neq 0$$

it its found that ω_E is identical to ~0 for the range of separations considered. The values computed for $\langle E_1E_2\rangle_\Theta$ are shown on Figure 10. The conclusion seems to be that the dust is uncorrelated in the 'circular sense' at least. This may be understandable from the dust distribution found in

the previous section. When the dust is confined to filaments with density variations, e.g. Figure 2 and 3, 'any' reddening may be found for 'any' small separation. Note that $\omega_E \neq 0$, $\Theta=0$, which implies that the number of clouds per unit length may be found from the method of moments: $k=1$ kpc^{-1} compared to $k = 4$-8 kpc^{-1} in the plane.

An uncorrelated dust distribution's influence on the galaxy distribution function is not evident but dust ripples as on Figure 2-8 will certainly have som effect on a homogeneous distribution of galaxies. With a reddening distribution as observed the autocorrelation function does not appear to be the best statistics to describe the spatial dust correlation. As the dust may be confined to strings a statistics sensitive to the orientation of the individual features may be thought of instead. It is emphasized that the conclusion stating that the dust is uncorrelated is preliminary, the reason for this proviso is that when the complete sample is used for calculating the excess products at a given angular separation, excesses from the whole distance range 50-600 pc are included and these excesses may not have any physical relationship. A calculation of the excess products from subsamples limited to excesses from narrow stellar distance intervals may give different results.

Small scale structure in the distribution of matter at high latitudes and the origin of the diffuse soft X-ray background

Since the surveys of the diffuse background at soft röntgen energies were completed an interesting conflict on the spatial location of the emission has come about. As the computed absorption cross section of the ISM gas, assuming a cosmic composition, only requires a few times 10^{20} atoms cm^{-2} to have an optical depth unity, the emission volumes are supposed to be within a few hundred pc. At the galactic poles this may not be the case. Ultraviolet absorption lines indicate the existence of plasmas with temperatures close to 10^5 K, Savage and de Boer (1981). Theoretical considerations on why high latitude clouds do not disperse on short timescales indicate that plasmas with even higher temperatures may be in pressure equilibrium with these clouds.

The consistency of a hot halo and the background emission has been studied within a two component emission model

$$I = I_L + I_R \exp(-\tau) \qquad (1)$$

where I_L signifies the intensity from a local unabsorbed emission and I_R the remote emission which will be absorbed by the intervening material with the effective optical depth τ.

τ is computed from atomic cross section, Cruddace et al. (1974), and the observed N_H columns. If the gas/dust ratio is known the optical depth may also be computed from the dust columns E(b-y). Dust column observations may be better to use than 21 cm observations because they relate specifically to the volumes from which the soft emission may be observed. But they introduce of course another parameter which is not well known either.

A plasma code at a given temperature is required to fit the three parameters I_L, I_R and σ_x to the observations I(l,b) and N_H(l,b). $\tau = \sigma_x N_H$, where σ_x is the effective cross section which may differ from the computed atomic cross sections because of a variable distribution of matter inside the beam of the X-ray experiment. The model values of σ_x in fact disagree with the atomic cross sections indicating either that the two component emission is not a proper model or that the matter obscuring the remote emission is not located in nice homogeneous sheets covering the complete X-ray beam.

Two obvious solutions to this problem have been proposed:

(a) There is only an insignificant if any remote soft X-ray emission. The local emission dominates the background.

(b) The absorbing gas has a discrete distribution and is clumped on scales much smaller than the X-ray beam.

The author may be prejudiced from his optical experiences but has a feeling that the (b) suggestion is to be preferred.

Recently a series of papers discussing inter alia the point (b) has appeared, Fried et al. (1980), McCammon et al. (1983), Jahoda et al. (1985). Jahoda et al. have performed new 21 cm observations to address specifically the problem of clumping on scales comparable to the X-ray beams. They have completed detailed mapping of the HI column density distribution in 20 randomly selected areas with a size $4°\times5°$. The X-ray beams have typically a FWHM of 7°, and are circular with a triangular response function.

The fit of the global observations to equation (1) requires that the effective absorption cross sections are reduced with approximately a factor of two. If the combined X-ray counts and column density data are to be reproduced the diminished absorption efficiency requires an ex-

treme degree of clumping, hence observations of the small scale distribution of matter is important. Twenty regions are mapped by Jahoda et al. with a spacing of only 10′ between the observations. The 140 foot telescope observations were corrected for side lobe effects by comparing a synthesized beam to the Crawford Hill beam for identical regions. The Crawford Hill survey, Stark et al. (1984) is supposed to be free from side lobe effects; conversely the telescope has a large beam: 90% of the intensity within 2°. Such a large beam may cause problems. Figure 9 showed that preferred separations of reddening pairs relating to lines of sight penetrating clouds are smaller than 30′. The cross section reduction is due to the difference of the average transmission over the beam, where the amount of matter may vary, from the transmission corresponding to the column density averaged over the beam

$$\alpha \equiv \frac{\sigma_{eff}}{\sigma_{atomic}} = \frac{-\ln\{\frac{1}{n}\Sigma\exp(-\sigma_{atomic} N_H)\}}{\frac{1}{n}\sigma_{atomic}\Sigma N_H} \qquad (2)$$

n is the numbeer of lines of sight observed in one of the 20 regions or in an area of comparable size.

The atomic cross section for the B-band (0.13-0.188 keV) and for the C-band (0.16-0.288 keV) is 1.75 10^{-20} cm^2/atom and 0.8 10^{-20} cm^2/atom respectively, McCammon et al. (1983). The effective cross sections resulting from the model fits are 0.65 10^{-20} and 0.52 10^{-20} cm^2/atom for the B and the C band respectively, Burrows et al. (1984). McCammon et al. op.cit. quote 0.37 10^{-20} and 0.40 10^{-20} cm^2/atom respectively.

Using the numbers by Burrows et al. requires reduction factors α_B=0.37 and α_C=0.65. The detailed mapping of the 20 regions resulted in reduction factors larger than 0.8 for the B-band as well as for the C-band, Jahoda et al. op.cit., Table 1. Obviously there is no evidence for the extreme gas clumping in the 140 foot observations and consequently little support for soft X-ray emission from a hot halo.

Two of the regions, 5 and 19, mapped by Jahoda et al. fall within the zone b > 70°. When the averages of the excess products were computed for various separations the polar cap was divided in 51 cells. The centers of the regions 5 and 19 are located in cell 42 and cell 15 respectively. The areas of cell 42 and 15 are 23.5 and 27.5 square degrees respectively and contain 95 and 103 lines of sight where the color excess E(b-y) was measured. Both area size and number of observing points are then comparable to the values from the radio survey. The reduction factor α for these two cells may be computed from the dust observations if the relationship between dust and gas was known, which it really is not. A

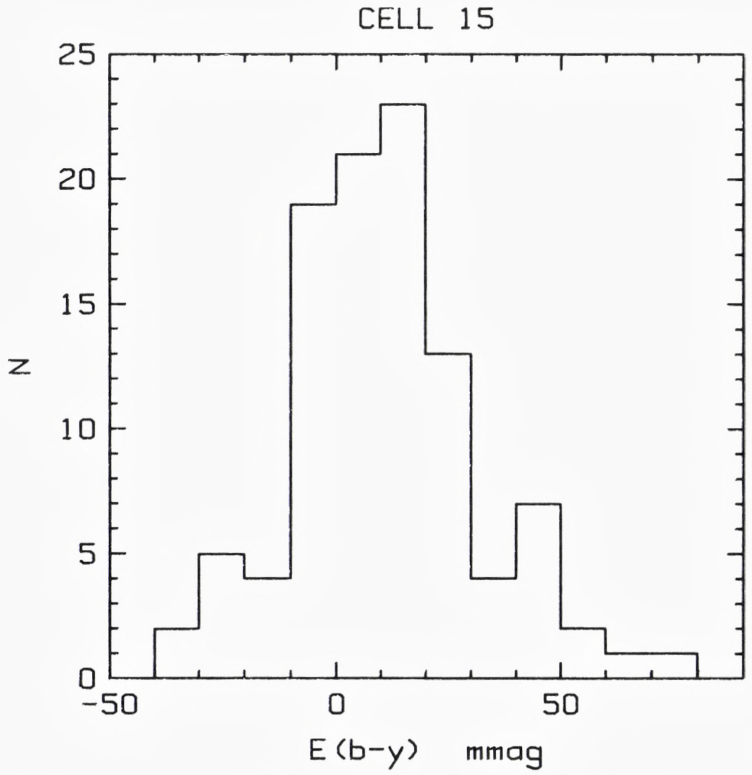

Fig. 11. Dust column distribution in cell 15, see Tabel 1. The histogram is assumed to be made up by observations of two components of the ISM. A truly diffuse part with $\langle E(b\text{-}y)\rangle = 0$ *and* $\sigma_{\langle E(b\text{-}y)\rangle} = 0.010$ *and a cloud part with* $E(b\text{-}y) > 0$. *See text for details.*

constant ratio is anyway assumed: $N_H/E(b\text{-}y) = 7.5\ 10^{21}\ cm^{-2}\ mag^{-1}$, Knude (1978).

Burstein and Heiles (1982) suggest a constant ratio above latitude +60°. Figure 11 is a histogram of the dust column distribution in cell 15. There is evidently a preponderance of positive excesses but also a well populated negative tail. For comparison Figure 12 shows a similar histogram for cell 5 which has the same latitude as cell 15 but $l_5 = l_{15} + 180°$. The distribution of dust columns in cell 5 is a beautiful specimen of the distribution of dust within a small area. Cell 5 has a slightly larger average excess than cell 15 but otherwise the two histograms are very similar. When computing the transmissions the negative excesses pose a problem. Negative excesses result from imperfect photometry. They are thought to result from observations of directions with very low dust

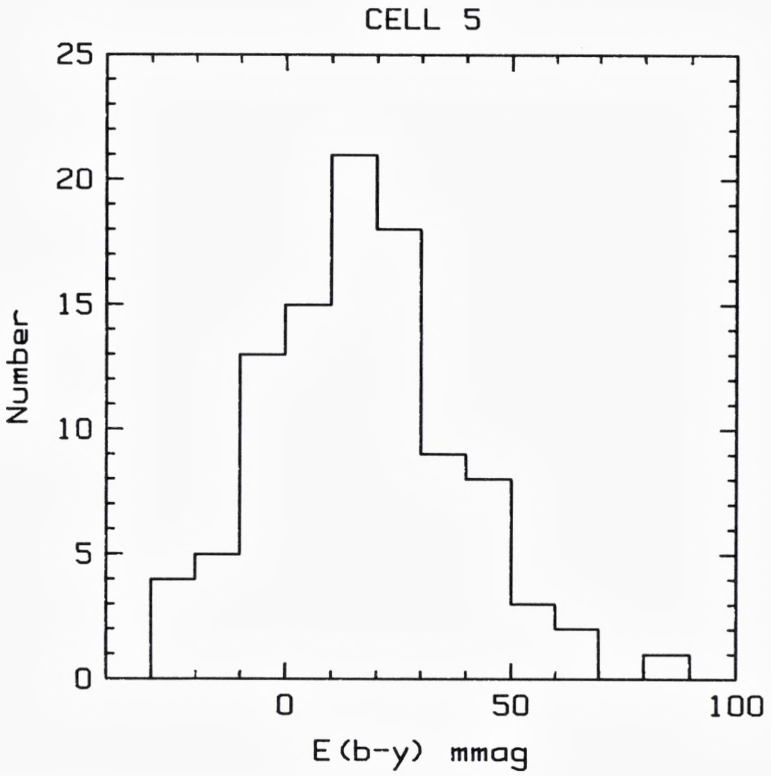

Fig. 12. Caption as to Figure 11, but for cell 5.

columns; the error distribution will then scatter about half of the actually zero reddenings below zero. Following this picture it is suggested that the interstellar dust is distributed on two basic components in the ISM: a truly diffuse part, the inter cloud medium (ICM), and a higher density part, the clouds. The transmission of the ICM is taken to be unity. In order to discriminate between the two components of the ISM in the computation of the reduction factors it is postulated that the ICM reddenings follow a gaussian with average excess ~0 and with a standard deviation 0.010 mag. The number of stars with excesses in the range from −0.01 to −0.020 equals accordingly the number of lines of sight scattered between one and two sigma below zero reddening. The total number of ICM lines of sight is then estimated from the number of stars in this excess interval. For the 99 lines of sight used in cell 5,43 is estimated to run exclusively in the transparent ICM. For the remaining 56 lines of sight individual transmissions are computed. An excess in the range from 0 to 0.030 may either be an ICM or a cloud line of sight. The

ICM lines are selected in sequence following the raster scan of the original observations.

For cell 5 the ratio of average transmission to the transmission for the average column is 0.3343 and 0.5581 for the B- and C-band respectively. The reduction factors computed for four cells are listed in Table 1. The factors depend naturally on the constancy of the gas/dust ratio. As briefly discussed previously this ratio seems to vary inside the pole region. The average N_H column estimated from the average dust column is a factor of two smaller than the average observed for region 5 and 19. The ratio $\langle N_H \rangle / \langle E(b\text{-}y) \rangle$ for these two regions are 1.48 10^{22} cm^{-2} mag^{-1} and 1.87 10^{22} cm^{-2} mag^{-1}. If the mean of these ratios replaces the gas/dust ratio used for cell 15 α_B, α_C drops to 0.167 and 0.332 respectively. The difference of the gas/dust ratio may be due to different distribution of gas with different temperatures relative to the dust distribution. The ratio

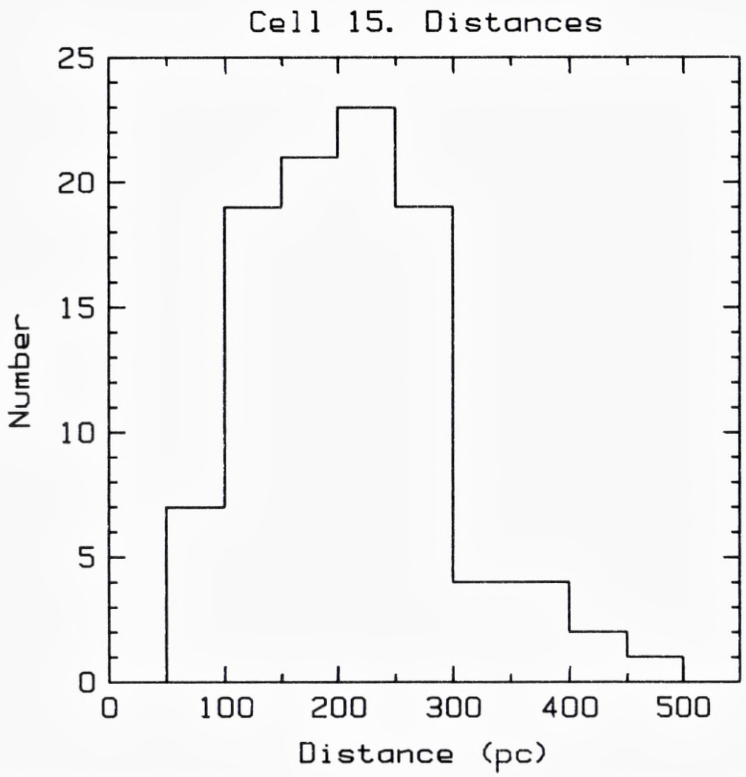

Fig. 13. Distribution of distances for the stars in cell 15. Note that the major part, ~75%, of the stars are beyond most estimates of the gas scale height.

Table 1. Reduction factors α_B,α_C for the B(0.13-0.188 keV) and C(0.16-0.288 keV) band absorption cross sections computed frem color excesses assuming a constant gas/dust ratio.

Cell	l	b	α_B	α_C	$\langle E(b-y) \rangle$	N
	(°)	(°)			mag	
42	36- 72	80-85	0.3456	0.5985	0.0066	95
5	72- 90	70-75	0.3343	0.5581	0.0166	101
15	252-270	70-75	0.3280	0.5315	0.0106	103
47	216-252	80-85	0.3593	0.5706	0.0117	123

Table 2. Reduction factors of the B and C band absorption cross sections from the observed gas column densities. The last column is the expected neutral hydrogen column density calculated from the observed dust columns assuming the standard gas/dust ratio.

Cell	Region	l	b	α_B	α_C	$\langle N_H \rangle$	$\langle E_H \rangle$
		(°)	(°)			10^{20} cm^{-2}	
42	5	59	84	0.934	0.970	0.98	0.495
15	19	264	71	0.959	0.981	1.98	0.795

7.5 10^{21} cm^{-2} mag^{-1} was estimated from observations in directions where HI was observed in absorption.

Table 1 contains the computed reduction factors for four high latitude cells. The radio results for the factors in region 5 and 19 (cell 42 and 15) are presented in Table 2. The dust data indicate extreme clumping but the radio data do not. For the four regions the average reductions are $\alpha_B = 0.34 \pm 0.01$ and $\alpha_C = 0.56 \pm 0.03$ in reasonable agreement with the requirements $\alpha_B = 0.37$ and $\alpha_C = 0.65$ required by the two component models. The dust data thus lend some support to the possibility of a diffuse contribution from a hot halo whereas the radio data do not. The reason for this discrepancy is not obvious. The computed average HI columns for region 5 and 19 in Table 2 are however lower than the average of the observed column densities by the factor of two as mentioned. This deviation is not caused by the limited distance range probed by the optical observations. Figure 13 shows the distribution of stellar

distances or the length of the lines of sight along which the dust is accumulated for cell 15. More than 75% of the stars are beyond 150 pc and then well above one scale height from the plane. If the four cells are compared to the same regions on the Hat Creek maps the E(b-y) predictions of the column densities are low with a factor 3-4 except for cell 5 where the agreement is better. Cell 5 contains the 21 cm maximum of the NGP zone.

As the computation of the E(b-y) values was completed very recently and none of them have been published so far it is thought appropriate to present a table with some of the data. Table 3 contains E(b-y) and distances of the stars in cell 15 where the center of region 19 is located.

As in the previous section it is a difficult matter to state a clear definitive conclusion concerning the small scale structure in the matter at high latitudes. The picture appears more complex than ever. But: part of the ism does clump on the scales required by the two component emission/absortion model for the diffuse soft X-ray background indicating that a significant fraction of the high latitude emission may originate in a hot halo. This conclusion is strongly depending on the assumed gas/dust ratio. To complicate matters further this ratio seems to differ from a previous derivation when formed from gas only seen in emission.

Table 3. Stars in the cell 15 (l: 252°-270°, b: 70°-75°). A star labelled with a DM number followed by a capital letter indicates that it is not in the Bonner Durchmusterung and that the nearest DM star is as indicated.

DM	l^{II}	b^{II}	E(b-y)	D
	DEG	DEG	MAG	PC
10 2380	269.5687	69.7660	0.011	258.8
11 2422	266.7675	70.3590	0.028	174.2
11 2423	267.4446	70.2027	0.044	190.7
11 2424	266.9501	70.5486	0.010	81.0
11 2424 A	267.2786	70.4969	0.028	283.3
11 2426	268.0995	70.2245	0.009	142.8
11 2426 A	267.4739	70.6108	0.016	245.1
11 2427	267.4739	70.6108	0.053	207.9
11 2431	269.1553	70.6877	0.007	133.1
12 2403	262.3851	69.7749	0.006	372.4
12 2408	262.1716	70.5662	−0.024	144.1

DM	l^{II}	b^{II}	E(b-y)	D
	DEG	DEG	MAG	PC
12 2409	262.0745	70.8151	0.048	119.5
12 2410	263.0046	70.4566	−0.022	291.3
12 2411	262.2965	70.7903	−0.001	158.9
12 2413	263.8512	70.2970	−0.020	214.6
12 2417	264.5242	71.0918	−0.024	191.2
12 2418	265.1323	71.0754	0.009	280.4
12 2421	266.0522	70.8070	−0.023	84.8
12 2423	267.0181	71.2336	−0.029	423.3
12 2425	267.4096	71.5542	0.018	261.7
12 2426	267.5265	71.6416	0.014	339.2
12 2427	267.6868	71.6855	0.009	138.1
12 2428	268.8782	71.3211	−0.008	102.5
12 2430	268.1942	71.8948	0.049	139.9
13 2464	254.7128	69.8715	−0.004	357.5
13 2470	257.5502	70.2124	−0.001	279.3
13 2472	257.5490	70.8621	−0.004	242.6
13 2476 A	258.3956	70.8920	0.007	238.7
13 2476	258.4571	70.9756	0.013	185.8
13 2478	259.4741	71.1262	0.053	165.4
13 2481	260.6036	71.6086	0.013	173.6
13 2482	261.9072	71.1325	0.006	128.3
13 2484	261.9296	71.7696	0.035	158.0
13 2485 A	262.1574	71.8126	0.010	263.5
13 2485	262.1237	71.7200	0.019	91.5
13 2487	263.5303	72.4348	0.030	210.5
13 2490	265.1486	71.9236	−0.006	249.5
13 2492	265.3295	72.2481	0.016	161.2
13 2494	265.4537	72.2514	0.012	176.4
13 2495 A	266.5759	72.1208	0.007	456.9
13 2495	265.9141	72.3075	−0.011	273.2
13 2498	266.3042	72.4669	−0.008	193.5
13 2500	267.4013	72.5564	0.001	277.2
13 2502	268.1752	72.5650	−0.003	127.3
13 2503	267.8181	73.1204	−0.004	116.8
13 2504	268.3594	73.0410	0.008	291.3
13 2505	268.6227	73.1537	0.041	170.7

DM	l^{II}	b^{II}	E(b-y)	D
	DEG	DEG	MAG	PC
13 2507 A	268.8483	73.3887	−0.003	267.8
13 2511	269.9527	73.6486	0.067	170.8
14 2438	252.4147	69.8136	0.020	112.6
14 2440	253.5935	70.0971	0.011	265.0
14 2441	253.6926	70.4236	0.023	150.4
14 2442	254.4439	70.1688	0.022	171.2
14 2447	254.3482	71.2410	0.025	106.4
14 2448	254.4727	71.4473	0.020	74.6
14 2448 A	254.1811	71.4062	0.011	297.4
14 2449	255.5264	71.2346	0.009	219.5
14 2451	256.0976	71.1995	0.022	127.1
14 2454	256.9979	71.4241	0.009	151.1
14 2455	257.8257	71.1506	0.001	277.6
14 2457	256.6912	71.9274	0.037	74.9
14 2458	256.9754	72.1582	0.037	142.3
14 2461	258.5009	72.1640	−0.011	694.0
14 2462	259.8231	71.7770	0.015	158.5
14 2465	259.2378	72.1510	0.016	215.5
14 2466	258.7192	72.4401	0.017	195.9
14 2469	261.0262	72.5113	0.009	231.2
14 2470	261.6546	72.2748	−0.011	441.8
14 2472	261.5299	73.0822	−0.002	219.8
14 2473	262.9986	72.9610	−0.001	150.8
14 2476 F	263.2831	73.5220	−0.007	303.7
14 2477	266.2775	73.4953	−0.007	201.7
14 2478	266.6203	73.5812	0.004	133.6
14 2481	267.3817	73.3631	0.001	104.3
14 2482	267.0350	73.6792	−0.003	266.9
15 2386 A	252.7008	70.9734	0.002	242.6
15 2394 A	254.0706	71.9882	−0.033	363.5
15 2394	253.6795	71.9275	0.020	393.1
15 2396	253.1113	72.3000	0.029	287.3
15 2398	254.5440	72.0121	0.049	145.4
15 2399	253.5880	72.6166	0.042	134.5
15 2400 A	255.6022	72.9178	−0.031	556.5
15 2401	256.3252	73.1577	−0.004	337.1

DM	l^{II}	b^{II}	E(b-y)	D
	DEG	DEG	MAG	PC
15 2403	257.0716	73.2121	−0.010	210.1
15 2405	257.9796	73.2490	0.007	155.2
15 2409	261.0343	73.3126	−0.023	201.9
15 2417 Q	261.4269	74.5105	0.018	282.4
15 2418	262.2001	74.2626	0.010	74.2
15 2419	262.5046	74.3499	0.015	195.7
15 2420	263.5779	74.1609	−0.009	217.1
15 2426	263.8356	74.9707	0.004	321.4
15 2427 A	265.8161	74.4124	0,018	262.3
15 2430 A	266.3453	74.8605	0.015	266.0
15 2430	266.6207	74.8690	0.010	215.0
15 2433	267.3352	74.8646	0.005	203.0
16 2325	254.4840	73.8025	0.021	238.7
16 2330	256.9201	73.7845	0.071	169.0
16 2331	257.1060	73.9820	0.024	259.4
16 2335	258.4148	74.0928	0.024	248.5
17 2423	252.6768	73.9673	0.043	247.4
17 2430	255.6209	74.6649	0.007	118.1

Concluding remarks

The incursion into the field of high latitude dust suggests a revision of three major points:

on the existence of high latitude dust: substantial amounts are present. The most reddened lines of sight are organized in a filamentous pattern.

on the autocorrelation of the dust distribution: apparently the dust is uncorrelated with the usual definition of the autocorrelation function. The variable obscuration may have other effects on the galaxy distribution than changing its amplitude and power. One could imagine that the galaxy distribution somehow was complementary to the dust distribution. A statistics sensitive to the orientation of the dust strings is required for such an investigation.

on the small scale dust distribution: the dust distribution in areas comparable in size to the beams applied in the soft X-ray surveys is found to show extreme clumping of a degree required to explain the reduced absorption cross section. If the dust and gas correlates spatially this result indicates that a fraction of the high latitude background may originate in the halo. It is however a serious question whether a general constant gas/dust ratio can be maintained. The NGP data indicates that rather large variations may be anticipated.

The dust investigations make up only part of the studies for which the NGP data were obtained. An immediate application will be the first estimates of density variations perpendicular to the galactic plane for various stellar subgroups.

ACKNOWLEDGEMENTS. *A photometric programme of proportions like the NGP survey may only be accomplished through the support from many individuals and authorities.*

T. Oja kindly made available the A and F star candidates of his spectral survey of the NGP zone before publication.

Experiences from Hβ photometry during periods with inferior sky conditions promted the development of a combined uvby-β photometer so repeated photometer changeovers could be avoided and observations continued even if clouds happens to rise. For faint stars it is also a great convenience that uvby-β photometry may be performed once the star has been identified. Observing efficiency has been improved significantly with this new generation of photometers. P. Bechman, R. Florentin and J. Klougart designed and built the photometer and aquisition system with much enthusiasm.

Observing time was granted by the Danish Astronomy Board, Stockholm University Observatory, KPNO and UNAM.

Thanks are due to F. Paresce for pointing out the possibilities of a cooperation with the San Pedro Martir Observatory, L. Carrasco for easing the way to San Pedro and to L. Rodriques for approving a Mexican-Danish cooperation in astronomy.

Financial support has been granted by the Danish Astronomy Board, the Danish Space Board, and the Danish Natural Science Research Council.

References

Burstein, D., Heiles, C.: 1978 Astrophys, J. *225,* 40
Burstein, D., Heiles, C.: 1982, Astron, J. *87,* 1165
Burrows, D. N., McCammon, D., Sanders, W. T., Kraushaar, W. L.: 1984, Astrophys. J. December 1 issue
Crawford, D. L., Mander, J.: 1966, Astron. J. *71,* 114
Crawford, D. L.: 1975, Astron. J. *80,* 955
Crawford, D. L.: 1978, Astron. J. *83,* 48
Crawford, D. L.: 1979, Astron. J. *84,* 1858
Cruddace, R., Paresce, F., Bowyer, S., Lampton, M.: 1974, Astrophys. J. *187,* 497
Davis, M., Groth, E. J., Peebles, J. E.: 1977, Astrophys. J. *212,* Letters 107
de Vaucouleurs, G., Buto, R.: 1983, Astron. J. *88,* 939
Fried, P. M., Nousek, J. A., Sanders, W. T., Kraushaar, W. L.: 1980, Astrophys. J. *242,* 987
Heiles, C.: 1975, Astron. Astrophys. Suppl. *20,* 37
Hill, G., Barnes, J. V., Hilditch, R. W.: 1982, Publ. dom. Astrophys. Obs. *XVI,* 111
Hill, G., Hilditch, R. W., Barnes, J. V.: 1983, Mon.Not.R. astr. Soc. *204,* 241
Jahoda, K., McCammon, D.., Dickey, J. M., Lockmann, F. J.: 1985, Astrophys. J., March 1 issue
Knude, J.: 1978, in Reiz, A., Andersen, T. (eds) 'Astronomical Papers Dedicated to Bengt Strömgren', 273
Knude, J.: 1979, Astron. Astrophys. Suppl. *38,* 407
Knude, J.: 1984, IAU Coll. 81, Kondo, Y., Bruhweiler, F. C., NASA Conference Publication *2345,* p. 123
McCammon, D., Burrows, D. N., Sanders, W. T., Kraushaar, W. L.: 1983, Astrophys. J. *269,* 107
Perry, C. L., Johnston, L.: 1982, Astrophys. J. Suppl. *50,* 451
Perry, C. L., Johnston, L., Crawford, D. L.: 1982, Astron. J. *87,* 1751
Sandage, A.: 1973, Astrophys. J. *183,* 711
Savage, B. D., de Boer, K. S.: 1981, Astrophys. J. *243,* 460
Seldner, M., Uson, J. M.: 1983, Astrophys. J. *264,* 1
Spitzer, L.: 1956, Astrophys. J. *124,* 40
Stark, A. A., Bally, J., Linke, R. A., Heiles, C.: 1984, in preparation
Strömgren, B.: 1966, Ann. Rev. Astron. Astrophys. *4,* 437